Molecular Crystals and Liquid Crystals Science and Technology. Section A. Molecular Crystals and Liquid Crystals

Publication details, including instructions for authors and subscription information:
http://www.tandfonline.com/loi/gmcl19

Syntheses and Crystal Structures of DBTTF Derivatives Substituted Unsymmetrically by Electron Donating Groups: $(MeO)_2(MDO)$ DBTTF, (EDO) (MDO) DBTTF and $(MeO)_2(EDO)$ DBTTF

T. Inayoshi [a] , K. Sato [a] , I. Miyazaki [a] , S. Yokoyama [a] & I. Ono [a]

[a] Department of Chemistry, College of Science and Engineering, Aoyama Gakuin University, Chitosedai, Setagaya-ku, Tokyo, 157, Japan

Version of record first published: 04 Oct 2006

To cite this article: T. Inayoshi, K. Sato, I. Miyazaki, S. Yokoyama & I. Ono (1998): Syntheses and Crystal Structures of DBTTF Derivatives Substituted Unsymmetrically by Electron Donating Groups: $(MeO)_2(MDO)$ DBTTF, (EDO) (MDO) DBTTF and $(MeO)_2(EDO)$ DBTTF, Molecular Crystals and Liquid Crystals Science and Technology. Section A. Molecular Crystals and Liquid Crystals, 309:1, 251-272

To link to this article: http://dx.doi.org/10.1080/10587259808045532

Mol. Cryst. Liq. Cryst., 1998, Vol. 309, pp. 251–272
Reprints available directly from the publisher
Photocopying permitted by license only

Syntheses and Crystal Structures of DBTTF Derivatives Substituted Unsymmetrically by Electron Donating Groups: $(MeO)_2$(MDO) DBTTF, (EDO) (MDO) DBTTF and $(MeO)_2$(EDO) DBTTF

TOMOKO INAYOSHI, KENGO SATO, ICHIRO MIYAZAKI, SAORI YOKOYAMA and ISAO ONO

Department of Chemistry, College of Science and Engineering, Aoyama Gakuin University, Chitosedai, Setagaya-ku, Tokyo 157, Japan

(Received 17 March 1997; In final form 20 July 1997)

Three novel unsymmetrically substituted DBTTF derivatives, $(MeO)_2$ (MDO) DBTTF, (EDO) (MDO) DBTTF, and $(MeO)_2$ (EDO) DBTTF, have been synthesized and their physicochemical properties are elucidated. Here, MeO, MDO, and EDO mean methoxy, methylenedioxy, and ethylenedioxy groups, respectively. Trimethylaluminum is found to be suitable for the syntheses of the above DBTTF derivatives using the non-coupling method. MDO is rather an effective substituent in reducing the difference between the first and the second redox potentials. The crystal structures of $(MeO)_2$ (MDO) DBTTF and $(MeO)_2$ (EDO) DBTTF were analyzed by an X-ray crystal structure analysis. In the crystal of $(MeO)_2$ (MDO) DBTTF, two molecules form a face-to-face pair, in which two molecules arrange so as to cancel their dipole moments to each other. The molecules of $(MeO)_2$ (EDO) DBTTF form a herringbone column structure in the crystal. Intermolecular short S··S atomic contacts are not found in the crystals of $(MeO)_2$ (MDO) DBTTF and $(MeO)_2$ (EDO) DBTTF. However, intermolecular interactions through C··C and C··O atomic contacts, and hydrogen bondings are recognized.

Keywords: Electron donor; synthesis; crystal structure; $(MeO)_2$(MDO) DBTTF; (EDO) (MDO) DBTTF; $(MeO)_2$(EDO) DBTTF

INTRODUCTION

The charge transfer (CT) complexes, formed between dibenzotetrathiafulvalene (DBTTF) and various organic and inorganic electron acceptors

(TCNQ,$TCNQCl_2$, $TCNQF_2$, $TCNQF_4$, $SnCl_6^{2-}$, $PtCl_6^{2-}$, etc.), have been synthesized, and their physicochemical properties, such as electrical or crystalographical properties, have been elucidated [1~6]. It is found, however, that the ability of DBTTF as an electron donor is not superior to that of TTF, though it has a more extended π-electronic system than TTF.

Although systematic works on the DBTTF CT complexes have been done to vary the kinds of the electron acceptors, there are few studies to modify the electron donor DBTTF. The introductions of strong electron donating groups into DBTTF are expected to promote its electron donating abilities and the formations of segregated stacking columns, leading to better conductive CT complexes. Thus, we have prepared the DBTTF derivatives, in which methoxy (MeO), methylenedioxy (MDO), and ethylenedioxy (EDO) groups are introduced symmetrically into the 5, 6, 5′, and 6′ positions of the DBTTF skeleton [7, 8]. In a previous investigation, a number of CT complexes of $(EDO)_2$ DBTTF (or BEDO-DBTTF) with various organic electron acceptors have been prepared, and their physicochemical properties have been clarified, where the EDO group introduced was suggested to play an important role in the formation of an assemble of self-aggregated donor through CH··O hydrogen bondings [8]. The above symmetrical DBTTF derivatives ($(MeO)_4$DBTTF, $(MDO)_2$DBTTF, and $(EDO)_2$(DBTTF)) are, however, not very soluble in ordinary organic solvents.

In the present investigation, in order to improve the electron donating properties and to increase the solubility of the DBTTF derivatives, we have attempted to prepare unsymmetrically substituted DBTTF derivatives, in which MeO, MDO, and EDO groups are introduced into both sides of DBTTF as shown below. Their redox potentials and crystal structures have also been determined.

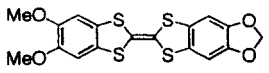

$(MeO)_2$(MDO)DBTTF

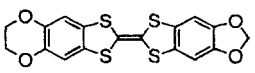

(EDO)(MDO)DBTTF

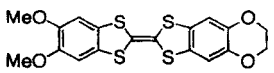

$(MeO)_2$(EDO)DBTTF

RESULTS AND DISCUSSION

Syntheses

For the preparations of the DBTTF derivatives treated here, two procedures can be considered, the methods of cross-coupling and non-coupling. Since the cross-coupling method gives three kinds of products whose isolation is

difficult, non-coupling method is adopted here [9]. For the non-coupling method, using trimethylaluminum as a Lewis acid at the key step, two routes (named as Routes A and B for each compound) can be considered as shown in Scheme 1, for a typical example of $(MeO)_2$ (MDO) DBTTF. As for the

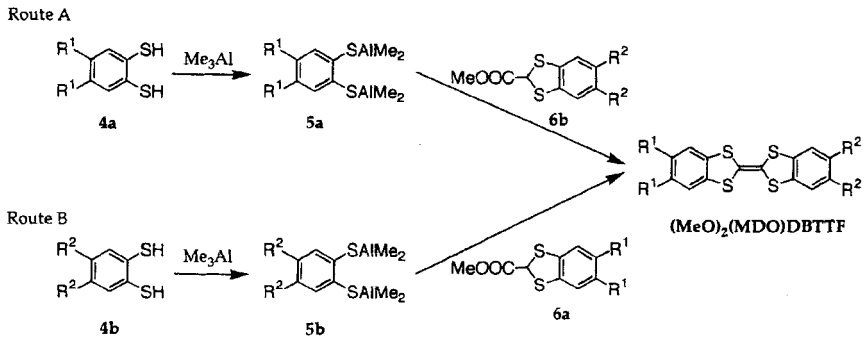

SCHEME 1 Preparation of (MeO_2) (MDO) DBTTF.

preparations of $(MeO)_2$ (MDO) DBTTF and $(MeO)_2$ (EDO) DBTTF, both routes were tested. Table I shows that Route B gave better results for $(MeO)_2$ (MDO) DBTTF, while Route A did for $(MeO)_2$ (EDO) DBTTF. The compound (EDO) (MDO) DBTTF was prepared using the ester (**6c**), since **6c** could be prepared in a better yield than **6b**. For the preparations of $(MeO)_2$ (MDO) DBTTF, (EDO) (MDO) DBTTF, and $(MeO)_2$ (EDO) DBTTF, the new compounds methyl 5,6-dimethoxy-1,3-benzodithiole-2-carboxylate (**6a**), methyl 5,6-methylendioxy-1,3-benzodithiole-2-carboxylate

TABLE I Non-coupling synthesis of unsymmetrical DBTTF derivatives

Entry	*Dithiols*	*Organoaluminium compounds*	*Esters*	*Products*	*Yields (%)*
1 (Route A)	4a	5a	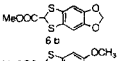	$(MeO)_2$ (MDO) DBTTF	6 0
2 (Route B)	4b	5b	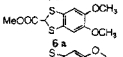	$(MeO)_2$ (MDO) DBTTF	7 0
3	4b	5b	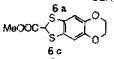	(EDO) (MDO) DBTTF	5 2
4 (Route A)	4c	5c	6a	$(MeO)_2$ (EDO) DBTTF	6 8
5 (Route B)	4a	5a	6c	$(MeO)_2$ (EDO) DBTTF	2 5

6b, and methyl 5,6-ethylenedioxy-1,3-benzodithiole-2-carboxylate (**6c**) were prepared.

As expected, the solubility in 1,1,2-trichloroethane of the three unsymmetrically substituted DBTTF derivatives considerably increases compared with that of symmetrically substituted DBTTF. The solubility for these compounds decreases in the order: $(MeO)_2$ (EDO) DBTT > $(MeO)_2$ (MDO)DBTTF ≈ (EDO) (MDO) DBTTF, though not being determined quantitatively.

Electronic Absorption Spectra

The electronic absorption spectra of the newly prepared three compounds together with that of DBTTF, measured in 1,1,2-trichloroethane, are shown in Figure 1. DBTTF, taken as a reference, shows intense absorption bands at 289, 311, and 349, and a weak broad band at 432 nm. $(MeO)_2$(MDO) DBTTF exhibits intense absorption bands at 303.5, 325 and 353, and very weak bands at 442 and 469 nm. The corresponding bands for (EDO) (MDO) DBTTF are found at 301.5, 325, 356, 436 and 468 nm, and for $(MeO)_2$(EDO) DBTTF at 301.5, 325, 353, 437 and 463 nm. The lowest energy band of DBTTF is red-shifted significantly by the introduction of the

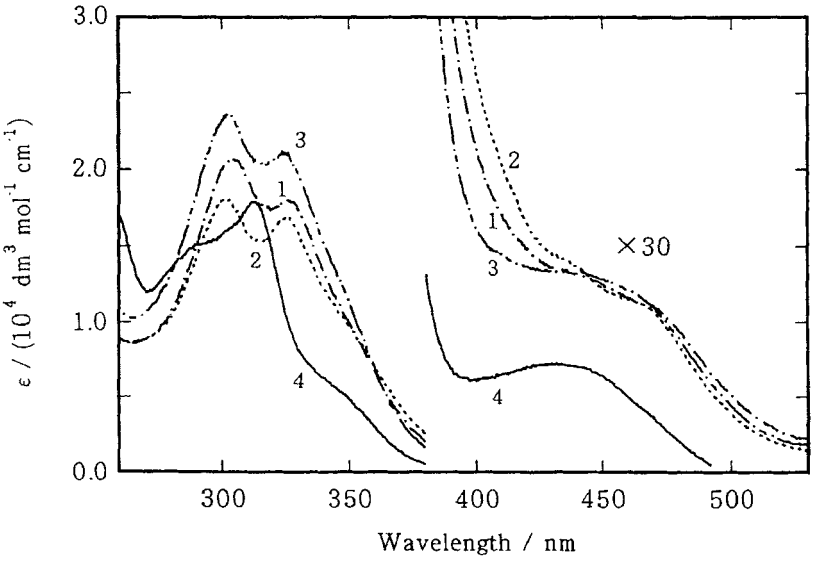

FIGURE 1 The electronic absorption spectra of $(MeO)_2$ (MDO) DBTTF (1:–·–·–), (EDO) (MDO) DBTTF (2:·····), $(MeO)_2$(EDO) DBTTF (3:–··–), and DBTTF (4:——) in 1,1,2-trichloroethane.

substituents, splitting into two shoulder bands. The corresponding absorption bands of the symmetrically substituted DBTTF derivatives in the same solvent are as follws. $(MeO)_4$DBTTF: 304, 325, 416, 444.5, and 467.5 nm. $(MDO)_2$DBTTF: 303.5, 326.5, 355, 444, and 470 nm. $(EDO)_2$DBTTF: 299.5, 323, 348, 437, and 471 nm [7]. It is seen that the symmetrically and unsymmetrically substituted DBTTF derivatives do not show much difference in the absorption spectra.

The PPP calculation shows that the main contributors to the exited state wavefunction corresponding to the observed 289 nm band of DBTTF are the excited configurations from HOMO to LUMO and/or higher vacant orbitals [10]. Thus, from the position of the corresponding absorption peak of each substituted DBTTF derivative, the relative strength of the electron donating power of the substituents may be inferred. According to the locations of the most intense bands at around 300 nm of the three symmetrically substituted DBTTF derivatives cited above, the electron donating strengths of the substituents are in the order of MeO > (or $\approx$) MDO > EDO, where two MeO groups are taken to be equivalent to one MDO or EDO group. The inference is in harmony with the similar data for unsymmetrically substituted DBTTF derivatives, the additivity of substituent effect being roughly assumed.

Cyclic Voltammetry

Table II shows the redox potentials (the first and the second half-wave potentials, $E_{1/2(1)}$ and $E_{1/2(2)}$), and the differences ($\Delta E = E_{1/2(2)} - E_{1/2(1)}$) of these unsymmetrical DBTTF derivatives, together with those of DBTTF and its symmetrically substituted derivatives. All the redox processes are found to be reversible; the separation between oxidation and reduction peak potentials in each pair of waves is 60 mV. From the viewpoints of redox potentials $E_{1/2(1)}$ and $E_{1/2(2)}$ (Tab. II), the electron donating strengths of the

TABLE II Redox potentials of DBTTF derivatives[a)]

Donor	$E_{1/2(1)}/V$	$E_{1/2(2)}/V$	$\Delta E/V$[b)]
$(MeO)_2$ (MDO) DBTTF	0.43	0.81	0.38
(EDO) (MDO) DBTTF	0.49	0.85	0.36
$(MeO)_2$ (EDO) DBTTF	0.44	0.85	0.41
DBTTF	0.64	1.06	0.42
$(MeO)_4$ DBTTF	0.41	0.79	0.38
$(MDO)_2$ DBTTF	0.48	0.83	0.35
$(EDO)_2$ DBTTF	0.50	0.90	0.40

a) The half-wave redox potentials vs. SCE, Pt electrode, 0.1M Bu_4NClO_4 in CH_2Cl_2, scan rate 200 mV/s, at 22 ± 1°C.
b) $\Delta E = (E_{1/2(2)} - E_{1/2(1)})$.

substitutents are in the order of MeO > MDO > EDO, which is the same as that found in the electronic absorption spectra. As for the unsymmetrically substituted DBTTF derivatives, both $E_{1/2(1)}$ and $E_{1/2(2)}$ are intermediate between those of the two corresponding symmetrically substituted DBTTF derivatives. It seems that, in this case, the substitution effects on the redox potentials are approximately additive.

Generally, ΔE is related to the intramolecular on site Coulomb repulsion energy, and give us useful criterions of the donors [11]. The values of ΔE of the symmetrically substituted DBTTF derivatives, shown in Table II, increase in the order: $(MDO)_2$ DBTTF < $(MeO)_4$ DBTTF < $(EDO)_2$ DBTTF. The values of ΔE of the unsymmetrically substituted DBTTF derivatives increase in the order: (EDO)(MDO)DBTTF < $(MeO)_2$(MDO) DBTTF < $(MeO)_2$(EDO)DBTTF. It is seen that the substituent MDO is rather effective on decreasing the ΔE value.

Crystal Structure

The crystal data, the data collection, and the refinement parameters are summarized in Table III.

TABLE III Crystal data, data collection and reduction parameters for $(MeO)_2$(MDO) DBTTF and $(MeO)_2$(EDO) DBTTF

	$(MeO)_2$ (MDO) DBTTF	*$(MeO)_2$ (EDO) DBTTF*
Formula	$C_{17}H_{12}O_4S_4$	$C_{18}H_{14}O_4S_4$
Formula wt	408.50	422.55
Crystal dimention	0.20×0.15×0.10 mm^3	0.10×0.10×0.25 mm^3
Crystal system	monoclinic	monoclinic
Space group	$P2_1/c$(#14)	$P2_1$(#4)
a/Å	14.687(4)	15.303(4)
b/Å	8.202(2)	4.140(2)
c/Å	14.482(4)	14.408(4)
β/deg	107.29(2)	107.32(2)
V/Å^3	1665.7(8)	871.3(5)
Z	4	2
Dcalc, g/cm^3	1.63	1.61
Diffractometer	Mac Science MXC18	Mac Science MXC18
Radiation	MoKα(λ=0.71073 Å)	MoKα(λ=0.71073 Å)
Scan mode	2 θ–ω	2 θ - ω
2 θ_{max}/deg	55	55
No. of intensity measured	4385	2442
Criterion for obsd.reflection	$\|F_0\| \geq 3\sigma\|F_0\|$	$\|F_0\| \geq 3\sigma\|F_0\|$
Reflections used in L.S.	2645	1855
No. of refined parameters	274	281
R	0.0351	0.0330
R_w	0.0471	0.0515
Counting statics weights of the form	$w=\exp[1.0\sin^2\theta/\lambda^2]/[\sigma^2(F_0)+0.002(F_0)^2]$	$w=\exp[1.0\sin^2\theta/\lambda^2]/[\sigma^2(F_0)+0.005(F_0)^2]$
goodness of fit	1.87	1.50

$(MeO)_2$ (MDO) DBTTF

Figure 2 ((a), (b) and (c)) illustrates ORTEP drawings of $(MeO)_2$ (MDO) DBTTF molecule together with the atom numbering. The central tetrathioethylene plane and the benzene ring with a methylenedioxy group are almost coplanar, while the benzene ring with two methoxy groups is not coplanar with the central tetrathioethylene, i.e., the dihedral angle between the planes of the central tetrathioethylene and the benzene ring substituted by methylenedioxy group and two methoxy groups are 178° and 174.5°, respectively as depicted in Figure 2(b). Two bond axes , O(1)—C(7) and O(3)—C(9), are bent downward from the benzene ring by 17° and 14°,

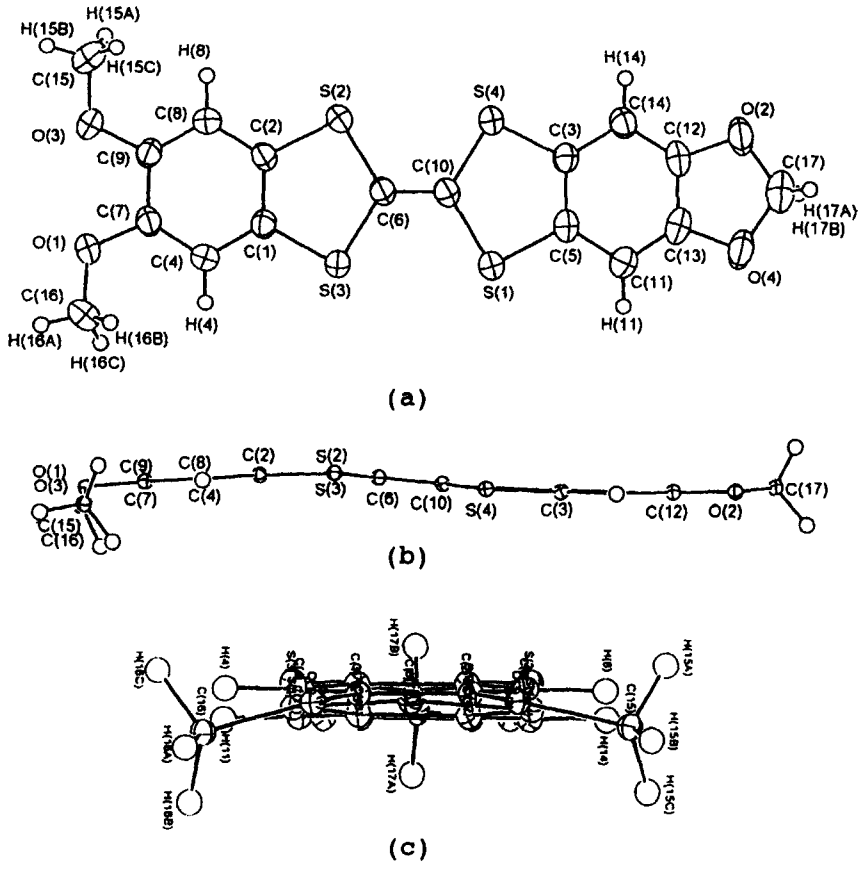

FIGURE 2 ORTEP drawing of $(MeO)_2$ (MDO) DBTTF: (a) the front view, (b) side view of (a), (c) viewed along the C(6)—C(10) bond axis.

respectively (Fig. 2(b)). Interatomic distances and bond angles for $(MeO)_2$(MDO) DBTTF appear in Table IV and the positional parameters are given in Table V. The crystal of $(MeO)_2$ (MDO) DBTTF does not have the column structure as seen from Figure 3(a) and (b). Two $(MeO)_2$(MDO) DBTTF molecules, in the crystal, form a face-to-face pair, in which two molecules arrange so as to cancel their dipole moments to each other. Two adjacent pairs are arranged perpendicularly to each other. The interplanar distance within the pair is ca. 3.58 Å. Within the pair, the $(MeO)_2$(MDO)

TABLE IV Interatomic Distances and Angles in $(MeO)_2$ (MDO) DBTTF

Atoms	*Dist. (Å)*	*Atoms*	*Dist.(Å)*
S(1)–C(5)	1.757(3)	S(1)–C(10)	1.752 (3)
S(2)–C(2)	1.752(3)	S(2)–C(6)	1.754(3)
S(3)–C(1)	1.756(3)	S(3)–C(6)	1.760(3)
S(4)–C(3)	1.754(3)	S(4)–C(10)	1.758(3)
O(1)–C(7)	1.372(4)	O(1)–C(16)	1.414(5)
O(2)–C(12)	1.381(4)	O(2)–C(17)	1.419(5)
O(3)–C(9)	1.372(4)	O(3)–C(15)	1.418(5)
O(4)–C(13)	1.381(4)	O(4)–C(17)	1.424(5)
C(1)–C(2)	1.382(4)	C(1)–C(4)	1.398(4)
C(2)–C(8)	1.390(4)	C(3)–C(5)	1.389(4)
C(3)–C(14)	1.401(4)	C(4)–C(7)	1.378(4)
C(5)–C(11)	1.409(4)	C(6)–C(10)	1.347(4)
C(7)–C(9)	1.404(4)	C(8)–C(9)	1.374(4)
C(11)–C(13)	1.361(5)	C(12)–C(13)	1.378(4)
C(12)–C(14)	1.363(4)		
Atoms	*Angle(°)*	*Atoms*	*Angle(°)*
C(5)–S(1)–C(10)	95.4(2)	C(2)–S(2)–C(6)	95.2(2)
C(1)–S(3)–C(6)	94.9(2)	C(3)–S(4)–C(10)	95.3(2)
C(7)–O(1)–C(16)	117.0(3)	C(12)–O(2)–C(17)	105.4(3)
C(9)–O(3)–C(15)	117.0(3)	C(13)–O(4)–C(17)	105.1(3)
S(3)–C(1)–C(2)	117.1(2)	S(3)–C(1)–C(4)	123.0(2)
C(2)–C(1)–C(4)	119.9(3)	S(2)–C(2)–C(1)	116.8(2)
S(2)–C(2)–C(8)	122.4(3)	C(1)–C(2)–C(8)	120.7(3)
S(4)–C(3)–C(5)	116.9(2)	S(4)–C(3)–C(14)	122.0(3)
C(5)–C(3)–C(14)	121.1(3)	C(1)–C(4)–C(7)	119.1(3)
S(1)–C(5)–C(3)	116.7(2)	S(1)–C(5)–C(11)	121.5(3)
C(3)–C(5)– C(11)	121.8(3)	S(2)–C(6)–S(3)	115.5(2)
S(2)–C(6)–C(10)	122.0(3)	S(3)–C(6)–C(10)	122.5(3)
O(1)–C(7)–C(4)	124.5(3)	O(1)–C(7)–C(9)	114.6(3)
C(4)–C(7)–C(9)	120.8(3)	C(2)–C(8)–C(9)	119.7(3)
O(3)–C(9)–C(7)	115.1(3)	O(3)–C(9)–C(8)	125.2(3)
C(7)–C(9)–C(8)	119.7(3)	S(1)–C(10)–S(4)	115.7(2)
S(1)–C(10)–C(6)	122.8(3)	S(4)–C(10)–C(6)	121.5(3)
C(5)–C(11)–C(13)	115.4(3)	O(2)–C(12)–C(13)	109.8(3)
O(2)–C(12)–C(14)	127.6(3)	C(13)–C(12)–C(14)	122.7(3)
O(4)–C(13)–C(11)	127.0(3)	O(4)–C(13)–C(12)	110.1(3)
C(11)–C(13)–C(12)	122.9(3)	C(3)–C(14)–C(12)	116.1(3)
O(2)–C(17)–O(4)	109.4(3)		

TABLE V Positional and Equivalent Isotropic Thermal parameters for $(MeO)_2$(MDO) DBTTF

Atom	*x/a*	*y/b*	*z/c*	*U(iso)*[a]
S(1)	0.15068(5)	0.02490(10)	0.45837(5)	0.044
S(2)	−0.11356(5)	0.30759(9)	0.36117(5)	0.040
S(3)	−0.02274(5)	0.07093(9)	0.26039(5)	0.039
S(4)	0.05651(5)	0.25994(10)	0.55679(5)	0.042
O(1)	−0.33392(14)	0.09759(27)	−0.02932(14)	0.048
O(2)	0.35820(15)	0.19973(32)	0.85612(14)	0.054
O(3)	−0.41105(14)	0.30229(28)	0.05763(14)	0.049
O(4)	0.43103(15)	0.01496(32)	0.77937(16)	0.055
C(1)	−0.13708(17)	0.14115(32)	0.19666(17)	0.033
C(2)	−0.17926(19)	0.25141(32)	0.24349(17)	0.034
C(3)	0.16708(18)	0.18168(33)	0.62533(18)	0.036
C(4)	−0.18649(19)	0.08732(35)	0.10368(19)	0.038
C(5)	0.21151(18)	0.07267(32)	0.57924(18)	0.035
C(6)	−0.01850(18)	0.17389(32)	0.36823(18)	0.035
C(7)	−0.27735(18)	0.14475(34)	0.06031(18)	0.036
C(8)	−0.2708(2)	0.3094(3)	0.1993(2)	0.039
C(9)	−0.31988(18)	0.25709(34)	0.10791(19)	0.037
C(10)	0.05379(18)	0.15455(32)	0.45030(18)	0.037
C(11)	0.3018(2)	0.0060(4)	0.6263(2)	0.042
C(12)	0.29925(19)	0.16790(37)	0.76410(19)	0.040
C(13)	0.34289(18)	0.05899(36)	0.71837(20)	0.041
C(14)	0.2112(2)	0.2316(4)	0.7207(2)	0.040
C(15)	−0.4647(3)	0.3845(6)	0.1102(3)	0.064
C(16)	−0.3070(3)	−0.0457(5)	−0.0688(3)	0.056
C(17)	0.4430(3)	0.1104(6)	0.8643(3)	0.061
H(4)	−0.1578(19)	0.0086(35)	0.0751(20)	0.036(7)
H(8)	−0.301(2)	0.385(4)	0.230(2)	0.041(8)
H(14)	0.186(2)	0.307(4)	0.753(2)	0.041(8)
H(11)	0.331(2)	−0.068(4)	0.596(2)	0.044(9)
H(16A)	−0.354(2)	−0.067(4)	−0.125(2)	0.050(9)
H(15A)	−0.438(3)	0.488(5)	0.125(3)	0.06(1)
H(16B)	−0.294(3)	−0.133(5)	−0.022(3)	0.07(1)
H(16C)	−0.246(3)	−0.025(4)	−0.087(2)	0.06(1)
H(15B)	−0.526(3)	0.396(4)	0.070(3)	0.06(1)
H(15C)	−0.463(3)	0.326(5)	0.171(3)	0.08(1)
H(17A)	0.453(3)	0.039(6)	0.922(3)	0.11(2)
H(17B)	0.491(3)	0.182(5)	0.863(3)	0.07(1)

a) $U_{iso} = 1/3\ (\Sigma\Sigma U_{ij} a_i^* a_j^* a_i a_j)/Å^2$

DBTTF molecules show no short contact less than the van der Waals (vdW) sum [12], but the molecules exhibit some short contacts with the molecules of the adjacent pairs: O(1)··H(17B) (2.67 Å: vdW sum = 2.72 Å), S(2)··H(16C) (2.90 Å: vdW sum = 3.00 Å), C(3)··H(16C) (2.80 Å: vdW sum = 2.90 Å), C(3)··C(16) (3.30 Å: vdW sum = 3.40Å), and O(1)··C(17) (3.18 Å: vdW sum = 3.22 Å) (Fig. 3 (b)). There are, however, no short S··S atomic contacts: the observed 3.72 ~ 3.79 Å distances exceed its vdW sum of

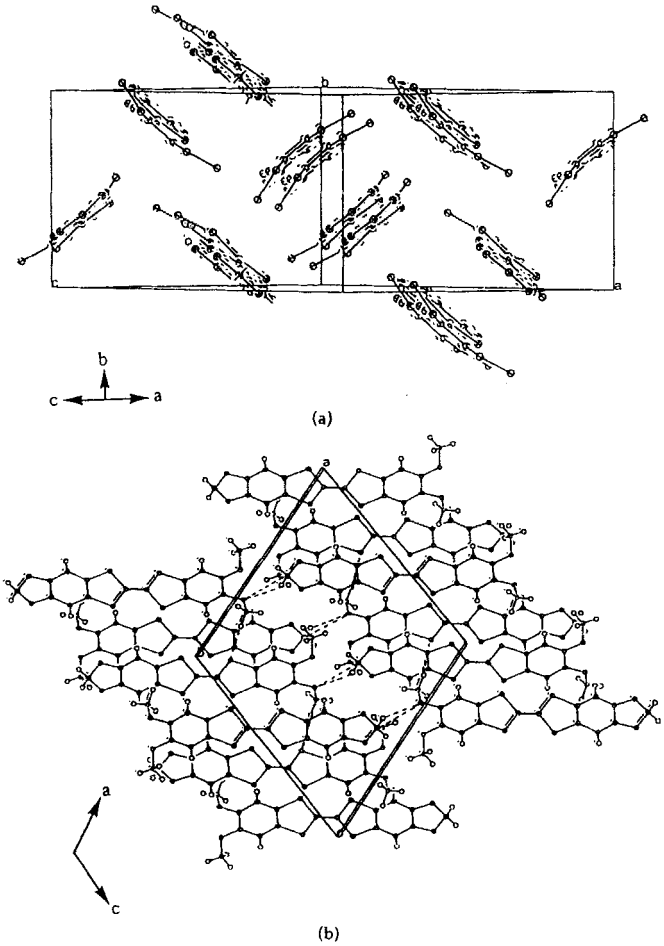

FIGURE 3 Crystal structure of $(MeO)_2$ (MDO) DBTTF: (a) viewed along the line bisecting the angle between *a*-axis and *c*-axis; (b) viewed along the *b*-axis, the dotted lines indicate intermolecular-interatomic short contacts.

3.60 Å. It may be worth to note that, in the formation of the intermolecular hydrogen bonding, one methoxy oxygen O(1) acts as a hydrogen acceptor, and the H (17B) atom of the methylenedioxy group acts as a donor, but the oxygen atom of the methylenedioxy group does not act as a hydrogen acceptor. $(MeO)_2$ (MDO) DBTTF has unsymmetrically substituted polar groups (see Fig. 2), which lead to intermolecular dipole–dipole interaction stabilizing the crystal structure.

$(MeO)_2$ (EDO) DBTTF

Figure 4((a), (b) and (c)) shows ORTEP drawings of $(MeO)_2$ (EDO) DBTTF molecule together with the atom numbering. The molecule is bent at the four sulfur atoms of the TTF skeleton to form a boat shape (Fig. 4 (b)). Both benzene planes are bent 7.9° and 10.9°, respectively, at the junctions to the central TTF plane; the bending angles are larger than those of the symmetrical BEDO-DBTTF molecule (6.4°, 7.5°) by ca. $2 \sim 3°$ and considerably smaller than those of BEDO-TTF molecule (21.5°, 24.6°). The carbon atoms of the two methoxy groups are in the plane of the benzene ring (Fig. (4c)). Two methylenes in the ethylenedioxy group take a staggered conformation. The interatomic distances and the bond angles for $(MeO)_2$ (EDO) DBTTF appear in Table VI, and the positional parameters in Table VII. The compound $(MeO)_2$ (EDO) DBTTF forms a herringbone packing, as in the case of DBTTF [3], along the b-axis shown in Figure 5(a).

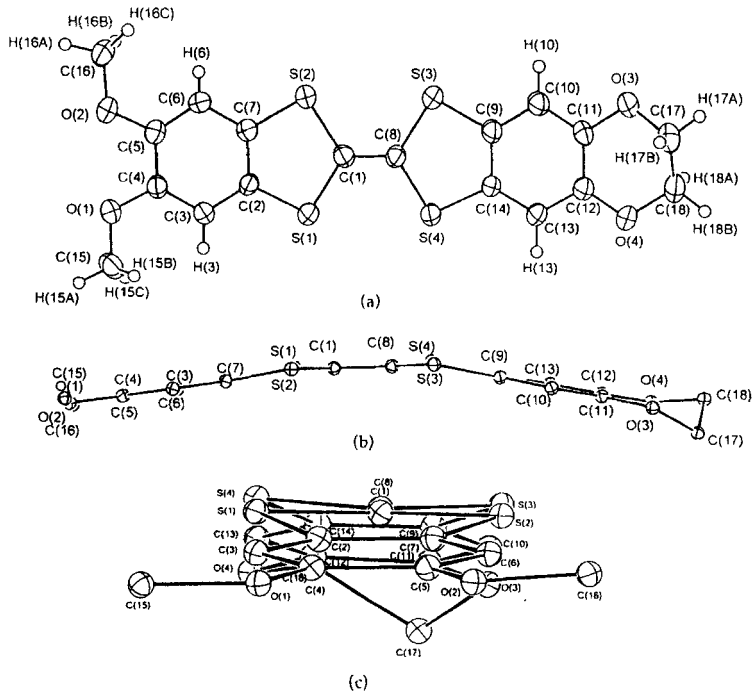

FIGURE 4 ORTEP drawing of $(MeO)_2$ (EDO) DBTTF: (a) the front view, (b) side view of (a), (c) viewed along the C(1)—C(8) bond axis.

TABLE VI Interatomic Distances and Angles in $(MeO)_2$ (EDO) DBTTF

Atoms	*Dist.(Å)*	*Atoms*	*Dist.(Å)*
S(1)–C(1)	1.756(5)	S(1)–C(2)	1.754(4)
S(3)–C(8)	1.758(5)	S(3)–C(9)	1.760(5)
S(2)–C(1)	1.760(5)	S(2)–C(7)	1.757(5)
S(4)–C(8)	1.753(5)	S(4)–C(14)	1.758(4)
O(2)–C(5)	1.364(5)	O(2)–C(16)	1.421(7)
O(4)–C(12)	1.378(6)	O(4)–C(18)	1.445(7)
O(1)–C(15)	1.419(7)	O(1)–C(4)	1.371(5)
O(3)–C(11)	1.385(5)	O(3)–C(17)	1.443(7)
C(1)–C(8)	1.344(6)	C(2)–C(7)	1.380(6)
C(2)–C(3)	1.387(6)	C(14)–C(13)	1.388(6)
C(14)–C(9)	1.395(6)	C(10)–C(11)	1.383(6)
C(10)–C(9)	1.387(6)	C(7)–C(6)	1.403(6)
C(11)–C(12)	1.401(6)	C(12)–C(13)	1.380(6)
C(6)–C(5)	1.376(7)	C(3)–C(4)	1.391(6)
C(17)–C(18)	1.481(7)	C(5)–C(4)	1.400(7)
Atoms	*Angle(°)*	*Atoms*	*Angle(°)*
C(1)–S(1)–C(2)	95.1(2)	C(8)–S(3)–C(9)	94.7(3)
C(1)–S(2)–C(7)	95.1(2)	C(8)–S(4)–C(14)	95.2(2)
C(5)–O(2)–C(16)	117.2(4)	C(12)–O(4)–C(18)	112.9(4)
C(15)–O(1)–C(4)	116.6(4)	C(11)–O(3)–C(17)	112.2(4)
S(1)–C(1)–S(2)	115.1(3)	S(1)–C(1)–C(8)	121.2(4)
S(2)–C(1)–C(8)	123.6(4)	S(1)–C(2)–C(7)	117.0(3)
S(1)–C(2)–C(3)	122.1(4)	C(7)–C(2)–C(3)	120.9(4)
S(3)–C(8)–S(4)	115.1(3)	S(3)–C(8)–C(1)	123.3(4)
S(4)–C(8)–C(1)	121.6(4)	S(4)–C(14)–C(13)	123.5(4)
S(4)–C(14)–C(9)	116.1(3)	C(13)–C(14)–C(9)	120.4(4)
C(11)–C(10)–C(9)	119.5(4)	S(2)–C(7)–C(2)	116.8(3)
S(2)–C(7)–C(6)	123.4(4)	C(2)–C(7)–C(6)	119.8(4)
O(3)–C(11)–C(10)	117.2(4)	O(3)–C(11)–C(12)	122.5(4)
C(10)–C(11)–C(12)	120.3(4)	O(4)–C(12)–C(11)	121.9(4)
O(4)–C(12)–C(13)	117.8(4)	C(11)–C(12)–C(13)	120.2(4)
C(7)–C(6)–C(5)	119.6(5)	C(14)–C(13)–C(12)	119.5(5)
C(2)–C(3)–C(4)	119.4(4)	S(3)–C(9)–C(14)	116.8(3)
S(3)–C(9)–C(10)	123.0(4)	C(14)–C(9)–C(10)	120.1(4)
O(3)–C(17)–C(18)	110.4(5)	O(2)–C(5)–C(6)	124.8(5)
O(2)–C(5)–C(4)	114.9(4)	C(6)–C(5)–C(4)	120.4(4)
O(1)–C(4)–C(3)	123.8(4)	O(1)–C(4)–C(5)	116.3(4)
C(3)–C(4)–C(5)	119.9(4)	O(4)–C(18)–C(17)	111.4(5)

The interplanar distance between the two neighboring molecules in the column is ca. 3.55 Å (Fig. 5(c)). This distance is shorter than that in the case of DBTTF where no intermolecular interaction exists [3]. Intermolecular atomic distances less than vdW distance are seen at O(3)··H(17B) (2.36 Å: vdW sum = 2.72 Å) and C(4)··H(15B) (2.80 Å: vdW sum = 2.90 Å) in Figure 5(c). These weak interatomic interactions may be regarded as a kind of hydrogen bondings. It is interesting that the hydrogen atom of the benzene ring acts as a hydrogen donor in the hydrogen bonding. Similarly,

TABLE VII Positional and Equivalent Isotropic Thermal Parameters for $(MeO)_2$(EDO) DBTTF

Atom	*x/a*	*y/b*	*z/c*	*U(iso)*[a]
S(1)	−0.06647(7)	0.18200	0.31433(7)	0.044
S(3)	0.21619(7)	−0.15591(50)	0.37499(7)	0.041
S(2)	0.02805(7)	−0.16073(51)	0.19081(7)	0.042
S(4)	0.11473(6)	0.17851(51)	0.49274(7)	0.043
O(2)	−0.2688(2)	−0.011(12)	−0.0986(2)	0.048
O(4)	0.4200(2)	0.4271(11)	0.7513(2)	0.050
O(1)	−0.3481(2)	0.3107(12)	0.0090(2)	0.047
O(3)	0.51836(19)	0.11630(103)	0.63451(21)	0.043
C(1)	0.0358(3)	0.0160(13)	0.3041(3)	0.038
C(2)	−0.1263(3)	0.1450(13)	0.1904(3)	0.035
C(8)	0.1127(3)	0.0179(14)	0.3795(3)	0.036
C(14)	0.2346(2)	0.1733(14)	0.5410(3)	0.035
C(10)	0.3769(3)	0.0000(14)	0.5176(3)	0.041
C(7)	−0.0830(3)	−0.0179(12)	0.1331(3)	0.036
C(11)	0.4237(2)	0.1366(13)	0.6060(3)	0.037
C(12)	0.3758(3)	0.2868(13)	0.6631(3)	0.039
C(6)	−0.1289(3)	−0.0705(12)	0.0344(3)	0.040
C(13)	0.2815(3)	0.3073(16)	0.6303(3)	0.042
C(3)	−0.2149(3)	0.2594(12)	0.1517(3)	0.041
C(9)	0.2822(3)	0.0170(13)	0.4851(3)	0.036
C(15)	−0.3923(3)	0.4843(16)	0.0672(4)	0.052
C(17)	0.5606(3)	0.3431(17)	0.7107(3)	0.048
C(5)	−0.2171(3)	0.0400(13)	−0.0043(3)	0.038
C(4)	−0.2605(3)	0.2084(13)	0.0538(3)	0.037
C(16)	−0.2308(3)	−0.1914(17)	−0.1590(3)	0.048
C(18)	0.5150(3)	0.3325(21)	0.7881(4)	0.054
H(6)	−0.102(3)	−0.162(14)	−0.001(3)	0.02(1)
H(3)	−0.245(3)	0.379(13)	0.186(3)	0.02(1)
H(16A)	−0.271(3)	−0.212(15)	−0.219(4)	0.04(1)
H(16B)	−0.210(3)	−0.395(15)	−0.131(4)	0.04(1)
H(13)	0.247(3)	0.415(16)	0.667(4)	0.06(2)
H(18A)	0.521(3)	0.087(13)	0.809(3)	0.03(1)
H(10)	0.408(3)	−0.090(14)	0.484(3)	0.04(1)
H(16C)	−0.170(4)	−0.119(21)	−0.159(4)	0.08(2)
H(17A)	0.625(3)	0.258(13)	0.733(3)	0.04(1)
H(18B)	0.538(4)	0.452(16)	0.841(4)	0.05(2)
H(17B)	0.551(5)	0.568(25)	0.675(5)	0.11(3)
H(15A)	−0.45355	0.55683	0.03573	0.08(2)
H(15B)	−0.35565	0.67093	0.09253	0.04(1)
H(15C)	−0.39415	0.34733	0.12033	0.06(2)

[a] $U_{iso} = 1/3(\Sigma\Sigma U_{ij} a_i^* a_j^* a_i a_j)/\text{Å}^2$.

intercolumn hydrogen bondings are recognized at the positions, O(4)··H(15C) (2.65 Å), O(1)··H(18B) (2.60 Å), O(3)··H(10) (2.61 Å), and O(2)··H(17A) (2.70 Å) in Figure 5(b). These hydrogen bondings result in the formation of the herringbone column of the $(MeO)_2$ (EDO) DBTTF crystal. However, short S··S atomic contacts do not exist; the observed distances are 3.70 ~ 3.80Å. A similar hydrogen bonding formation is

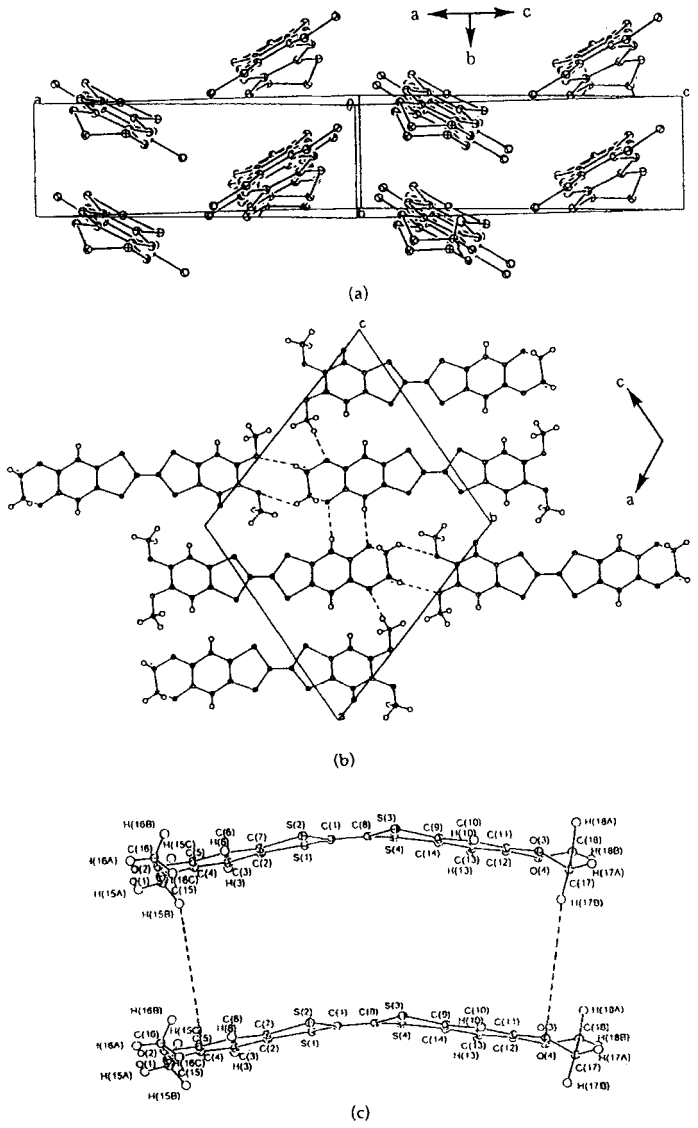

Figure 5 Crystal structure of $(MeO)_2$(EDO) DBTTF: (a) viewed along the line bisecting the angle between *a*-axis and *c*-axis; (b) viewed along the *b*-axis, intermolecular short contacts are shown by dotted lines; (c) the short C-H···O contact within a donor stack is shown by dotted lines.

reported in the case of BEDO-TTF. In this molecule, intercolumn and intracolumn hydrogen bonding exist [13]. In the crystal of $(MeO)_2$ (EDO) DBTTF, the molecules form a column along the *b*-axis, in which

the molecules arrange obliquely with respect to the short molecular axis; this may reduce the intercolumn intermolecular repulsion. The angle between the short molecular axis and the ac-plane is ca. 30°. In this crystal, both intercolumn and intracolumn hydrogen bondings are formed, unlike the case of $(MeO)_2$ (MDO) DBTTF, in which hydrogen bondings only exist between the molecules of the adjacent pairs. It seems that the hydrogen bonding interactions between the oxygen atom (methoxy and ethylenedioxy groups) and the hydrogen atom (benzene ring, ethylenedioxy and methoxy groups), in $(MeO)_2$(EDO) DBTTF, contribute significantly to the stability of the crystal. Furthermore, the intercolumn-intermolecular dipole–dipole interactions may contribute to the stability of the crystal, the dipole moments being induced by the unsymmetrically substituted polar groups.

According to Whangbo *et al.*, the calculated energy of C-H··O interaction is comparable to the C-H··anion energy [14]. It is reported that the hydrogen bondings between the donor molecules enhance the ability of self-aggregation, which is favorable in the formation of segregated column structures in CT complexes [15].

EXPERIMENTAL

Measurements

^{1}H NMR spectra were recorded on a JEOL JNM-400 spectrometer (270 MHz) in $CDCl_3$ with TMS as an internal standard. Both low- and high-resolution mass spectra were taken using a JEOL JMS-SX102 mass spectrometer at 70 eV with EI method. UV-visible absorption spectra were measured in 1,1,2-trichloroethane with a Shimadzu UV-3101PC spectrophotometer. Cyclic voltammetric measurements were performed on a NPGS-301 potentiostat (Nikko Keisoku) in $0.04 \sim 0.1$ mM solutions of the donor and 0.1 M solutions of tetrabutylammonium perchlorate in dichloromethane with Pt working and counter electrodes vs. SCE at a scan rate of 200 mV/s and at 22 ± 1°C.

X-ray diffraction data were collected on an automatic four circle diffractometer at RT. The reflections were scanned at the rate of 10°/min in ω axis. Crystan-GM was used as the computer program for the solution and the refinement of the crystal structure, and the structure was solved by a direct method (SIR 92). The structure was refined using a full-matrix least-squares refinement with anisotropic thermal parameters for the non-

hydrogen atoms and isotropic ones for hydrogen atoms. The positions of hydrogen atoms were determined by differential syntheses.

Materials

Trimethylaluminum (Kanto Chemical Co., 1.02M, hexane solution), 1,2-dimethoxybenzene (Tokyo Kasei Chemical Industry Co.), 1,2-methylenedioxybenzene (Wako Pure Chemical Co.) and 1,4-benzodioxan (E. Merck Co.) were used as purchased.

Preparation of Benzendithioles (4a, b, c)

The preparations of the starting materials to benzenedithioles are illustrated in Scheme 2.

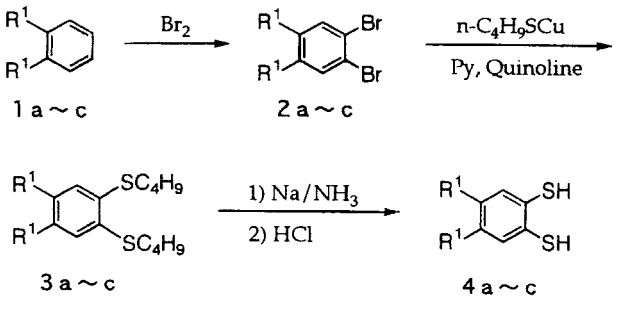

a : $R^1=R^1=MeO$
b : $R^1 \frown R^1=OCH_2O$
c : $R^1 \frown R^1=OCH_2CH_2O$

SCHEME 2 Preparations of benzenedithiol derivatives.

1,2-Dibromo-4,5-dimethoxybenzene (2a). The compound **2a** was synthesized by adding 160 g (1.0 mmol) of bromine in CCl_4 (100 ml) to a solution of 69.0 g (0.50 mmol) of 1,2-dimethoxybenzene in CCl_4 (200 ml) at $0 \sim 5°C$ over 3 h. The product was recrystallized from ethanol. Yield 90%; colorless plate; Mp $87 \sim 89°C$ (lit [16], $88 \sim 89°C$; ^1H NMR ($CDCl_3$) $\delta = 3.89$ (6H, s, OCH_3), 7.09 (2H, s, ArH); ^{13}C NMR ($CDCl_3$) $\delta = 55.9$ (quar, OCH_3), 114.3 (s, ArBr), 115.4 (d, ArH), 148.4 (s, ArOCH)$_3$; MS (EI) m/z 296 (M^+).

1,2-Bis (*n*-butylthio)-4,5-dimethoxybenzene (3a). Cuprous *n*-butylmercaptide was prepared by the method of Adams *et al.* [17]. The compund **3a** was prepared according to the literature [18]. The brown oily product was

distilled in vacuum to give a pale orange oil; Bp 193 ~ 197°C/0.4 mmHg. After standing for several days, the precipitated solid was recrystallized from ethanol. Yield 79%, Mp 56 ~ 58°C (lit [18], 57°C); ^{1}H NMR ($CDCl_3$) $\delta = 0.92$ (6H, t, CH_3), 1.47 (4H, six, $CH_2\underline{CH_2}\ CH_3$), 1.62 (4H, quin, $CH_2\underline{CH_2}\ CH_2$), 2.88 (4H, t, $S\underline{CH_2}\ CH_2$), 3.88 (6H, s, OCH_3), 6.90 (2H, s, ArH); MS (EI) m/z 315 (M^+).

4,5-Dimethoxy-1,2-benzenedithiol (4a). The same method as that used for o-benzenedithiol was employed [19]. The compund **4a** was prepared from **3a** (yield 76%). A pale yellow solid; Mp 60 ~ 61°C (lit [18], 62°C); ^{1}H NMR ($CDCl_3$) $\delta = 3.72$ (2H, s, SH), 3.84 (6H, s, OCH_3), 6.91 (2H, s, ArH); MS (EI) m/z 202 (M^+).

1,2-Dibromo-4,5-methylenedioxybenzene (2b). The compound **2b** was synthesized in the same way as **2a**: 400 g (2.1 mmol) of bromine in CCl_4 (120 ml) was added to a solution of 122 g (1.0 mmol) of 1,2-methylenedioxybenzene in CCl_4 (300 ml) at 0 ~ 5°C over 3h. The product was recrystallized from ethanol. Yield 82 %; colorless plate; Mp 83 ~ 84°C (lit [20], 86°C); ^{1}H NMR ($CDCl_3$) $\delta = 5.99$ (2H, s, OCH_2O), 7.05 (2H, s, ArH); MS (EI) m/z 280 (M^+).

1,2-Bis(*n*-butylthio)-4,5-methylenedioxybenzene (3b). To a mixture of dry quinoline (120 ml) and dry pyridine (12 ml), 32.6 g (120 mmol) of **2b** was added, and the solution was stirred and refluxed for 4 h at 150 ~ 170°C with 45.8 g (300 mmol) of a fresh cuprous *n*-butylmercaptide under N_2. After cooling to ca. 100°C, the reaction solution was poured into a mixture of ice (300 g) and conc. HCl (180 ml), and was stirred for about 1 h. The aqueous part was discarded by decantation, and the dark gummy residue was extracted with ether. The ether extract was washed twice with 10% HCl, once with H_2O, twice with conc. ammonium hydroxide, and with H_2O again. The organic solution was dried over potassium carbonate anhydride, and the ether was removed from the filtrate by evaporation. The brown oily residue was distilled in vacuum to give an orange oily product; Bp 130°C/2.0 mmHg (lit [20], 162~5°C/2.0 mmHg). The oil was purified by a silica gel chromatography, in which a mixture of chloroform and hexane was used as the eluent, giving a yellow oil. Yield 62%; ^{1}H NMR ($CDCl_3$) $\delta = 0.92$ (6H, t, CH_3), 1.38 ~ 1.51 (4H, six, $CH_2\underline{CH_2}CH_3$), 1.56~1.68 (4H, quin, $CH_2\underline{CH_2}CH_2$), 2.84 (4H, t, $S\underline{CH_2}CH_2$), 5.95 (2H, s, OCH_2O), 6.85 (2H, s, ArH); MS (EI) m/z 298 (M^+).

4,5-Methylenedioxy-1,2-benzendithiol (4b). The same method as for **4a** was used. A pale yellow solid of **4b** (3.5 g, 18.4 mmol) was obtained from 7.3 g

(24.5 mmol) of **3b** (Yield 75 %); Mp 82 ~ 83°C (lit [20], 86.5°C); ^{1}H NMR ($CDCl_3$) $\delta = 3.69$ (2H, s, SH), 5.89 (4H, s, OCH_2O), 6.89 (2H, s, ArH); MS (EI) m/z 186 (M^+).

1,2-Dibromo-4,5-ethylenedioxybenzene (2c), 1,2-bis(*n*-butylthio)-4,5-ethylenedioxybenzene (3c), and 4,5-ethylenedioxy-1,2-benzendithiol (4c).

The preparations of the materials **2c**, **3c** and **4c** are described in the literature [8].

As for the preparations of $(MeO)_2$ (MDO) DBTTF and $(MeO)_2$ (EDO) DBTTF, two methods, Routes A and B were employed (Tab. I).

Preparation of $(MeO)_2$ (MDO) DBTTF

Route A

Methyl 5,6-methylenedioxy-1,3-benzodithiole-2-carboxylate (6b). To a 20 ml benzene solution containing 1.49 g (8 mmol) of **4b** and 1.19 g (8 mmol) of methyl dichloroacetate, 1.62 g (16 mmol) of triethylamine was added dropwise at 0°C. After being kept for 3 h at RT, the white solid formed was filtered off. The solvent was evaporated under reduced pressure, and the obtained crystalline product was recrystallized from methanol to give a white solid **6b**. Yield 63%, Mp 69~70° C; ^{1}H NMR ($CDCl_3$) $\delta = 3.77$ (3H, s, $COOCH_3$), 5.25 (1H, s, CH), 5.95 (2H, s, OCH_2O), 6.78 (2H, s, ArH); MS (EI) m/z (rel intensity) 256 (M^+; 15), 197 (M^+-$COOCH_3$; 100). Found: m/z 255.9807 (M^+). Calcd for $C_{10}H_8O_4S_2$: M, 255.9812.

$(MeO)_2$ (MDO) DBTTF. In a two-necked flask, a solution of **4a** (0.20 g, 1 mmol) in 10 ml dry dichloromethane) was placed dropwise at 0°C under an argon atmosphere via a syringe, to which 1.85 ml (2 mmol) of trimethylaluminum (1.01 M hexane solution) was added dropwise. The solution was stirred for 1.5 h, to which saturated dichloromethane solution of ester **6b** (0.27 g, 1 mmol) was added without the isolation of bis (dimethylaluminum) dithiolate **5a**. After being further stirred for 15 h at RT, 0.3 g of $Na_2SO_4 \cdot 10H_2O$ was added in small pieces at 0°C. After the gas evolution had ceased (about 1 h at RT), the solution was dried over anhydrous Na_2SO_4. Evaporation of the solvent left an orange residue. Yield ca. 60 %; Mp 295 ~ 298°C; ^{1}H NMR ($CDCl_3$) $\delta = 3.74$ (6H, s, OCH_3), 6.06 (2H, s, OCH_2O), 7.22 (4H, s, ArH); MS (EI) m/z 408 (M^+). Found: C, 49.83; H, 2.94; S, 31.24 %. Calcd for $C_{17}H_{12}O_4S_4$: C, 49.98; H, 2.96; S, 31.39 %.

Route B

Methyl 5,6-dimethoxy-1,3-benzodithiole-2-carboxylate (6a). To a 20 ml benzene solution of 0.80 g (4 mmol) of **4a**, 0.60 g (4 mmol) of methyl dichloroacetate was added in the presence of triethylamine (0.81 g, 8 mmol). For details, see the synthesis of **6b**. The obtained product was recrystallized from methanol to give a white solid **6a**. Yield 69 %; Mp 103~104° C; ^{1}H NMR ($CDCl_3$) $\delta = 3.78$(3H, s, $COOCH_3$), 3.83 (6H, s, OCH_3), 5.25 (1H, s, CH), 6.78 (2H, s, ArH); MS (EI) m/z (rel intensity) 272 (M^+; 29), 213 (M^+ -$COOCH_3$; 100). Found: m/z 272.0164 (M^+). Calcd for $C_{11}H_{12}O_4S_2$: M, 272.0171.

$(MeO)_2$(MDO) DBTTF. Treatment of **4b** by trimethylaluminum, in a similar way as **4a** to give **5a** (Route A), gave bis(dimethylaluminum) dithiolate **5b**. The addition of the saturated dichloromethane solution of ester **6a** to **5b** gave a solid product in ca. 70 % yield, which was recrystallized from dimethylformamide. The obtained orange rhombic crystal was found to be the same as the product prepared in Route A. Then, the crystal structure was determined by X-ray analysis.

Preparation of (EDO) (MDO) DBTTF

Methyl 5,6-ethylenedioxy-1,3-benzodithiole-2-carboxylate (6c). By the same method used for the synthesis of **6a** or **6b**, the compound **6c** was synthesized, using **4c** as the starting material. The product was recrystallized from methanol. Yield 50 %; Mp 108~110°C; ^{1}H NMR ($CDCl_3$) $\delta = 3.76$ (3H, s, $COOCH_3$), 4.20 (4H, s, OCH_2CH_2O), 5.21 (1H, s, CH), 6.75 (2H, s, ArH); MS (EI) m/z (rel intensity) 270 (M^+; 20), 211 (M^+-$COOCH_3$; 100). Found: m/z 269.9987 (M^+) Calcd for $C_{11}H_{10}O_4S_2$: M, 270.0004.

(EDO) (MDO) DBTTF. The procedure used for the synthesis of $(MeO)_2$ (MDO) DBTTF was applied. The addition of 5.18 ml (5.60 mmol) of trimethylaluminum (1.01 M hexane solution) to 28 ml dry dichloromethane solution of **4b** (0.52 g, 2.80 mmol) gave bis (dimethylaluminum) dithiolate **5b**. Subsequent addition of the saturated dichloromethane solution of the ester **6c** (0.73 g, 2.7 mmol), without the isolation of **5b**, gave an orange product. The product was recrystallized from dichloromethane. Yield 52 %; Mp 294~297°C; ^{1}H NMR ($CDCl_3$) $\delta = 4.14$ (4H, s, OCH_2CH_2O), 5.89 (2H, s, OCH_2O), 7.19 (4H, s, ArH); MS (EI) m/z 406 (M^+). Found: C, 50.59; H, 2.61 %. Calcd for $C_{17}H_{10}O_4S_4$: C, 50.23; H, 2.48 %.

Preparation of $(MeO)_2$ (EDO) DBTTF

Route A

The preparation of the ester **6a** was described in Route B of $(MeO)_2$ (MDO) DBTTF.

$(MeO)_2$(EDO) DBTTF. The treatment was, in general, identical with that reported already in the case of (EDO) (MDO) DBTTF, except that **4c** was used instead of **4b**. Addition of the ester **6a** to **5c** gave the desired product, which was recrystallized from dimethylformamide. The orange needle crystal was obtained, then, the structure was determined by X-ray crystal structure analysis. Yield 68%; Mp 242~245°C; ^{1}H NMR ($CDCl_3$), $\delta = 3.84$ (6H, s, OCH_3), 4.23 (4H, s, OCH_2CH_2O), 6.78 (4H, s, ArH); MS (EI) m/z 422 (M^+). Found: C, 51.14; H, 3.41%. Calcd for $C_{18}H_{14}O_4S_4$: C, 51.16; H, 3.34 %.

Route B

The addition of **6c** to **5a** which was prepared by a similar treatment of **4a** (Entry 1 in Tab. I) with trimethylaluminum gave the same product $(MeO)_2$(EDO)DBTTF in 25% yield.

CONCLUSION

Three kinds of DBTTF derivatives substituted unsymmetrically by electron donating groups, $(MeO)_2$ (MDO) DBTTF, (EDO) (MDO) DBTTF, and $(MeO)_2$ (EDO) DBTTF, have newly been synthesized. Here, MeO, MDO, and EDO mean methoxy, methylenedioxy, and ethylenedioxy groups, respectively. The non-coupling method using $Al(CH_3)_3$ was adopted to avoid the formations of undesirable symmetrically substituted derivatives. The solubility of the above three compounds in organic solvents, such as 1,1,2-trichloroethane, is improved significantly compared with that of symmetrically substituted DBTTF derivatives. As for $(MeO)_2$ (EDO) DBTTF and $(MeO)_2$ (MDO) DBTTF, X-ray crystal structure analyses were performed. The crystal data are summerized in Table III. In the crystal of $(MeO)_2$ (MDO) DBTTF, two molecules form a pair so as to cancel their dipole moments to each other. The crystal of $(MeO)_2$ (EDO) DBTTF takes a herringbone structure. For $(MeO)_2$ (EDO) DBTTF, two kinds of intracolumn intermolecular hydrogen bondings are formed; one is between the oxygen and the hydrogen atoms of the adjacent EDO groups, and the other is between the aromatic carbon atom, linked with the MeO group, and

the hydrogen atom of the adjacent MeO group. These hydrogen bondings might be helpful in the formation of a segregated column structure in the crystal of charge transfer complexes with $(MeO)_2$ (EDO) DBTTF. The cyclic voltammetry measurements show that the $E_{1/2(1)}$ and $E_{1/2(2)}$values are intermediate between those of the corresponding two symmetrically substituted DBTTF derivatives.

Acknowledgements

The authors wish to thank Prof. Emeritus S. Matsumoto, Prof. T. Hoshi of Aoyama Gakuin University, and Prof. Y. Kanzaki of Showa College of Pharmaceutical Sciences for their helpful discussions.

References

[1] (a) H. Kobayashi and J. Nakayama, *Bull. Chem. Soc. Jpn.*, **54**, 2408 (1981); (b) T. J. Kistenmacher, T. J. Emge, F. M. Wiygul, W. A. Bryden, J. S. Chappell, J. P. Stokes, L-Y. Chiang and D. O. Cowan, *Solid State Commun.*, **39**, 415 (1981).
[2] C. S. Jacobsen, H. J. Pedersen, K. Mortensen and K. Bechgaard, *J. Phys. C*, **13**, 3411 (1980).
[3] T. J. Emge, F. M. Wiygul, J. S. Chappell, A. N. Bloch, J. P. Ferraris, D. O. Cowan and T. J. Kistenmacher, *Mol. Cryst. Liq. Cryst.*, **87**, 137 (1982).
[4] T. J. Emge, W. A. Bryden, F. M. Wiygul., D. O. Cowan, T. J. Kistenmacher and A. N. Bloch, *J. Chem. Phys.*, **77**, 3188 (1982).
[5] L. S. Veretennikova, R. N. Lyubovskaya, R. B. Lyubovskii, L. P. Rozenberg, M. A. Simonov, R. P. Shibaeva and M. L. Khidekel, *Dokle. Akad. Nauk SSSR*, **241**, 862 (1978).
[6] R. P. Shibaeva, L. P. Rosenberg and R. M. Lobkovskaya, *Kristallografiya*, **25**, 507 (1980).
[7] T. Inayoshi, *et al., unpublished data.*
[8] T. Senga, T. Kamoshida, L. A. Kushch, G. Saito, T. Inayoshi and I. Ono, *Mol. Cryst. Liq. Cryst.*, in press.
[9] T. Mori and H. Inokuchi, *Chem. Lett.*, **1992**, 1873.
[10] T. Hoshi, *private communication.*
[11] K. Takahashi, T. Nihira, K. Takase and K. Shibata, *Tetrahedron Lett.*, **30**, 2091 (1989).
[12] The van der Waals radii employed in this paper are as follows; C 1.70, H 1.20, N 1.55, O 1.52, S 1.80 Å.
A. Bondi, *J. Phys. Chem.*, **68**, 441 (1964).
[13] M. A. Beno, H. H. Wang, K. D. Carlson, A. M. Kini, G. M. Frankenbach, J. R. Ferraro, N. Larson, G. D. McCabe, J. Thompson, C. Purnama, M. Vashon and J. M. Williams, *Mol. Cryst. Liq. Cryst.*, **181**, 145 (1990).
[14] M.-H. Whangbo, D. Jung, J. Ren, M. Evain, J. J. Novoa, F. Mota, S. Alvarez, J. M. Williams, M. A. Beno, A. M. Kini, H. H. Wang and J. R. Ferraro, *The Physics and Chemistry of Organic Superconductors* edited by G. Saito, and S. Kagoshima, (Springer Proceedings in Physics 51, Springer, Berlin, 1990), 262–266.
[15] S. Horiuchi, H. Yamochi, G. Saito, K. Sakaguchi and M. Kusunoki, *J. Am. Chem. Soc.*, **118**, 8604 (1996).
[16] L. F. Tietze and Th. Eicher, *Reaktionen und Synthesen im Organischchemischen Praktikum und Forschungslaboratorium*, (Georg Thieme Verlag, Stuttgart-New York 1991).

[17] R. Adams, W. Reifschneider and A. Ferretti, *Org .Synth.*, Coll. V, 107.
[18] N. Wolki and G. Klar, *Phosphorus and Sulfur*, **36**, 261 (1988).
[19] A. Ferretti, *Org. Synth.*, Coll. V, 419.
[20] F. Dallacker and H. Zegers, *Ann. Chem.*, **689**, 156 (1965).